Proceedings of the ASME 2011 Dynamic Systems and Control Conference
DSCC2011
October 31 - November 2, 2011, Arlington, VA, USA

ON THE INFLUENCE OF COMPOSITION ON THE THERMALLY-DOMINANT RECOMPRESSION HCCI COMBUSTION DYNAMICS

Shyam Jade*, Erik Hellström, Anna Stefanopoulou
University of Michigan
Ann Arbor, Michigan 48109

Li Jiang
Robert Bosch Corporation
Farmington Hills, Michigan 48331

ABSTRACT

A zero dimensional, mean-value, control-oriented model for recompression homogeneous charge compression ignition (HCCI) combustion with two discrete states representing temperature and composition dynamics is presented. This model captures steady state magnitudes and trends in combustion phasing, residual gas fraction, and mass flows caused by sweeps in valve timings, fueling rate, and fuel injection timing. It is shown that the coupling of the composition state with the mainly thermally-driven combustion dynamics causes competing slow and fast dynamics that shape the transient response of the phasing. A decoupled version of the model, where composition does not affect combustion phasing, is also developed in an effort to further simplify the model. This version matches the steady state fidelity of the coupled model, but has a qualitatively different dynamical behavior. Both models exhibit complex behaviors such as limit cycles at extremely late phasing. Both realizations are valid contenders as low order steady state representations of HCCI behavior. High-fidelity transient data will be necessary to further clarify the necessity of including composition effects on combustion phasing.

NOMENCLATURE

a/bTDC	After / before top dead center
CA##	Crank angle at which ##% of fuel energy is released
EVO/C	Exhaust valve opening / closing
HCCI	Homogeneous charge compression ignition
i_{bd}	Inert gas fraction of blowdown gases
i_c	Inert gas fraction of charge before combustion
IVO/C	Intake valve opening / closing
m_f	Mass of fuel
NVO	Negative valve overlap
SOC	Start of combustion
SOI	Start of injection
p_α	In-cylinder pressure at event α
T_α	In-cylinder temperature at event α
T_{bd}	Temperature of blowdown gases
x_r	Residual gas fraction
ω	Engine speed, in RPM

*Address all correspondence to sjade@umich.edu

INTRODUCTION

A major challenge with homogeneous charge compression ignition (HCCI) engines is adequate combustion control. To enable model-based control approaches this contribution develops, validates, and analyzes control-oriented models.

Previous low-order model structures [1–5] are extended to obtain satisfactory estimation results over a fairly extensive data set from a four cylinder 2.0 liter gasoline engine with several actuator sweeps at one engine speed. Specifically, the energy losses during combustion are modeled as a function of the states and a semi-empirical model of the residual gas fraction is adapted from [2]. The influence of early fuel injection on combustion phasing is included through an Arrhenius expression. It is also shown that the charge composition influences the transient behavior due to the coupling between the composition and the thermal dynamics. This dynamic influence is investigated here, as earlier sensitivity analysis [6] showed that temperature at IVC is the dominant variable for capturing the steady state combustion phasing. Hence steady-state sensitivity is not sufficient to judge the necessity of including composition effects on combustion phasing.

To this end, we compare here two models, one where both temperature and composition influence combustion and a second where only the charge temperature affects combustion. The latter involves the tuning of less parameters and captures steady state combustion phasing as accurately as the former. We also show that both models are capable of predicting limit cycle behavior at

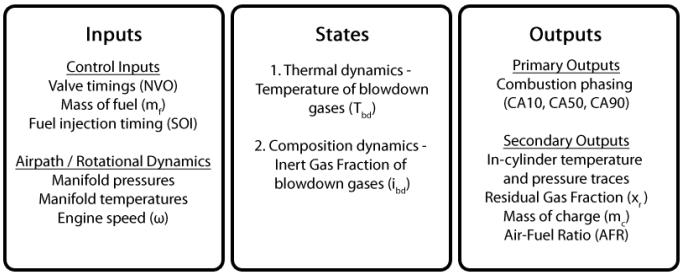

Figure 1. INPUT / OUTPUT MODEL OVERVIEW

conditions associated with late phasing. The dynamic response, however, of the two models is different. Namely, the temperature and composition influenced model exhibits overshooting response, whereas decoupling composition results in mostly damped behavior. Hence for effective controller design there is a need to understand and evaluate different model parameterizations that predict both steady state and transient behavior.

MODELING PROCESS

A control-oriented model that describes HCCI combustion must be sophisticated enough to capture all relevant physical trends, while being simple enough to enable effective controller design and analysis. This work deals with recompression HCCI [7], in which the exhaust valve is closed early and the intake valve is opened late, thus resulting in a negative valve overlap (NVO). The model developed is a discrete-time model with two states – (i) the temperature of the blowdown gases (T_{bd}), representing thermal dynamics and (ii) the inert gas fraction of the blowdown gases (i_{bd}), representing composition dynamics. An input / output overview of the model is presented in Fig. 1.

The actuator inputs considered are the negative valve overlap (NVO), the mass of fuel (m_f), the start of injection (SOI), and engine speed (ω). The valve timing is controlled by a cam phasing actuator with fixed cam profiles. The use of variable fuel injection timing shows promising results in HCCI combustion phasing control [5], both on a cycle-to-cycle and a cylinder-to-cylinder basis. Fuel injection in the recompression region causes thermal and chemical changes to the fuel due to the moderately high temperatures and pressures.

The primary output of the model is combustion phasing. This is quantified by the location of CA10, CA50 and CA90, which are the crank angles at which 10%, 50% and 90% respectively of the total heat release occur. A number of other important outputs are calculated such as the residual gas fraction (x_r), the in-cylinder Air-Fuel ratio (AFR_c), and the in-cylinder pressure and temperature traces.

Figure 2 shows a typical in-cylinder pressure trace for a recompression-based HCCI engine. Each engine cycle lasts for 720 °CA and is considered to end at EVO, that is after combustion finishes. In each cycle 0 °CA is considered to be at the combustion TDC. Figure 2 clearly shows the negative valve overlap resulting

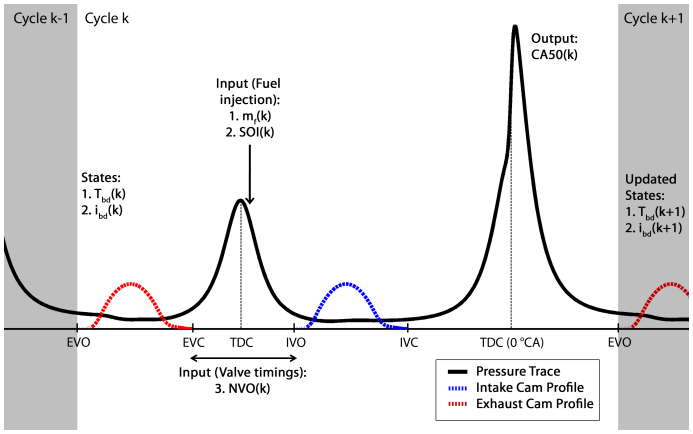

Figure 2. TYPICAL IN-CYLINDER PRESSURE TRACE

in a recompression region of moderately high temperatures and pressures, into which the fuel is injected at the desired time.

The parameters used in the model equations are fitted to experimental data. The nature of the dataset and the estimation results are presented in the section "Steady State Validation".

Residual Gas Fraction

The mass of charge in the cylinder (m_c) includes the mass of air and fuel inducted per cycle plus the residual mass (m_{res}) trapped from the previous cycle. The residual gas fraction (x_r) is defined as the ratio between m_{res} and m_c. A basis function for x_r was developed for rebreathing-based HCCI in [2] by emulating the engine as a pumping device. This has been adapted to the residuals trapped in recompression HCCI with good results, and is given in Equation (1)

$$x_r(k) = \left(\alpha_1 + \alpha_2 \left(\frac{\omega(k)}{2000}\right)^{\alpha_3} NVO(k)\right) \left(1 + \frac{\alpha_4 \left(\frac{p_{em}(k)}{p_{im}(k)}\right)^{\alpha_5}}{\sqrt{T_{bd}(k)}}\right) \quad (1)$$

where p_{im} and p_{em} are the pressures of the intake and exhaust manifold respectively.

Composition in the cylinder

The composition in the cylinder before and after combustion is shown in Fig. 3. At any point in the cycle, the charge in the cylinder is assumed to be a mixture of three components – air, fuel and inert gases. The chemical composition of these mixtures is determined from the stoichiometric combustion equation of the fuel considered. For example, from Eq. (17), which represents the stoichiometric combustion of one mole of iso-octane fuel, the constituents of the in-cylinder charge are considered to be:

1. Fuel (iso-octane) : C_8H_{18}
2. Air : $O_2 + 3.773N_2$
3. Inert gases : $8CO_2 + 9H_2O + 47.16N_2$

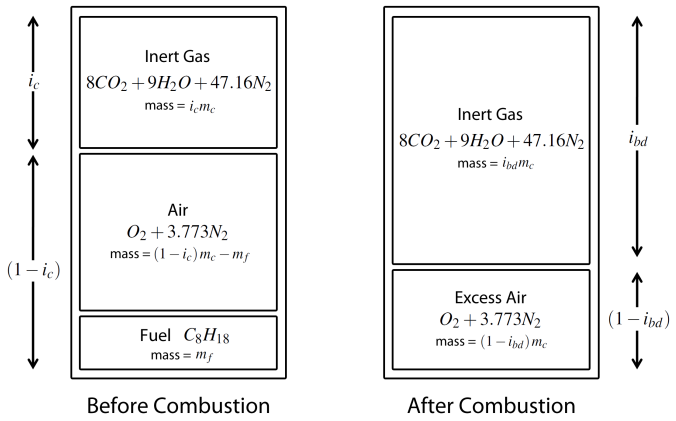

Figure 3. IN-CYLINDER COMPOSITION, BEFORE AND AFTER COMPLETE LEAN COMBUSTION

The inert gas fraction (IGF), which is defined to be the ratio of the mass of inert gases to the total mass of charge, is used to account for composition effects. Similar to [2], the IGFs before combustion (i_c) and after combustion (i_{bd}) are related to each other by Eq. (2) and (3).

$$i_c(k) = x_r(k) i_{bd}(k) \tag{2}$$

$$i_{bd}(k+1) = \left(\frac{AFR_s+1}{AFR_c(k)+1}\right)(1-i_c(k)) + i_c(k) \tag{3}$$

where $i_{bd}(k)$ is the IGF of the blowdown gases of the previous cycle. The air-fuel ratio in the cylinder before combustion (AFR_c) is described later by Eq. (5), while the stoichiometric AFR (AFR_s) is assumed to be 14.7. The composition of the residual gases is assumed to be the same as that of the blowdown gases. The state update equation for i_{bd}, presented in Eq. (4), can be derived from Eq. (2), (3), (5) and (7).

$$i_{bd}(k+1) = \frac{(AFR_s+1)\, m_f(k) R(x_r(k))}{p_{ivc}(k) V_{ivc}(k)} T_{ivc}(k) + x_r(k) i_{bd}(k) \tag{4}$$

where Eq. (10) and (9) give the dependence of $T_{ivc}(k)$ on $T_{bd}(k)$.

Relationship between i_{bd} and χ_{O_2} Instead of i_{bd}, the mole fraction of oxygen before combustion (χ_{O_2}) can be equivalently chosen as the composition state. This is shown in Appendix A, where the relationship between i_{bd} and χ_{O_2} is derived.

AFR before combustion (AFR_c) As external EGR is not used in this study, the fresh charge is assumed to consist purely of air. This considerably simplifies the comprehensive air charge model presented in [2]. The trapped residuals contain excess air that is left over after lean combustion. Both of these sources of air are considered while calculating AFR_c in Eq. (5). Relative AFR in the cylinder before combustion (λ_c) is calculated in Eq. (6).

$$AFR_c(k) = \frac{(1-i_{bd}(k)x_r(k))\, m_c(k)}{m_f(k)} - 1 \tag{5}$$

$$\lambda_c(k) = \frac{AFR_c(k)}{AFR_s} = \frac{(1-i_{bd}(k)x_r(k))\, m_c(k) - m_f(k)}{14.7 m_f(k)} \tag{6}$$

Mass of charge The mass of charge (m_c) is estimated by the ideal gas law. Here the gas constant varies with x_r.

$$m_c(k) = \frac{p_{ivc}(k) V_{ivc}(k)}{R(x_r(k))\, T_{ivc}(k)} \tag{7}$$

$$R(x_r(k)) = 274\,(1-x_r(k)) + 290 x_r(k) \tag{8}$$

State of Charge at IVC

Estimating the state of charge at IVC is critical to the accuracy of combustion phasing prediction, as the actuators have no control authority after IVC. Pressure at IVC (p_{ivc}) can be approximated as a linear function of the intake manifold pressure. Temperature at IVC (T_{ivc}) is calculated by a mass weighted average between temperatures of the fresh charge from the intake manifold (T_{im}) and the residual gases from the previous cycle's combustion (T_r) as shown in Eq. (10). Thermal effects of early injection on the temperature of the residuals are captured in Eq. (9) based on fuel injection timing and mass. Here $f_1(m_f(k), SOI(k))$ is a bilinear function that increases with larger and earlier fuel injection. This estimates the charge cooling effects of fuel vaporization, and possible heat release due to exothermic reactions.

$$T_r = T_{bd}(k) - f_1(m_f(k), SOI(k)) \tag{9}$$

$$T_{ivc}(k) = x_r(k) T_r + (1-x_r(k))\, T_{im}(k) \tag{10}$$

Combustion Process

The combustion is assumed to be complete if it is lean. For the effects of partial fuel burn at very late phasing or when close to stoichiometric levels, see [8, 9]. CA10 is considered to be the start of combustion (SOC) while CA90 is considered to be the end of combustion. The model is parameterized using experimental data to predict the temperature and pressure of the charge at important angles in the combustion process, such as CA10, CA50, CA90, and EVO. The intermediate regions between these points are assumed to be ideal polytropic or adiabatic processes to form complete pressure and temperature traces. The in-cylinder volume at any desired crank angle is given by standard cylinder geometry relations [10]. The combustion process starts at IVC and can be split into three phases – (1) a polytropic compression phase that leads to combustion, (2) a burn phase, and (3) a polytropic expansion phase followed by blowdown and exhaust.

Phase 1: IVC to SOC The start of combustion in the HCCI combustion process is determined by an Arrhenius rate reaction, given by Eq. (11) and (12). This is motivated by work such as [11] and the expression developed for the ignition time

delay for the autoignition of iso-octane in [12]. Sensitivity analysis of the autoignition integral in [6] suggests that temperature is the dominant factor in determining the start of combustion. Hence, Eq. (12) includes pressure and temperature effects only as a simplification in determining SOC. In [5], the effect of early fuel injection was captured by varying the Arrhenius threshold in the autoignition integral. A more physical strategy [13] considered in this study is to compute the autoignition integral given by Eq. (11) in the recompression region. This method is attractive as it provides a more physical basis function for parameterizing the phenomenon. Equation (11) is evaluated and the result is used as the initial value for the main combustion integral in Eq. (12), thus reducing the effective Arrhenius threshold.

$$\int_{SOI}^{IVO} A_{rc} p_c^{n_p} \left(\frac{m_f(k)}{m_c(k)}\right)^{n_f} \exp\left(\frac{-E_{a,rc}}{RT_c}\right) \frac{d\theta}{\omega(k)} = \xi \qquad (11)$$

$$\int_{IVC}^{CA10} A \left(p_{ivc}(k) \upsilon_{ivc}^{n_c}\right)^{n_p} \exp\left(\frac{-E_a \upsilon_{ivc}^{1-n_c}}{RT_{ivc}(k)}\right) \frac{d\theta}{\omega(k)} = 1-\xi \qquad (12)$$

Here $\upsilon_{ivc}(\theta)$ is defined as $\frac{V_{ivc}}{V_c(\theta)}$. In Eq. (11), the pressure (p_c) and temperature (T_c) in the cylinder are obtained by assuming a polytropic process from EVC to IVO with different constant polytropic exponents before and after SOI. The parameters A_x, n_x and E_x are parameterized using data.

Phase 2: Combustion Duration Combustion duration $(\Delta\theta)$ is defined to be the crank angle degrees between CA10 and CA90. In the operating regions considered, data shows that this can be modeled as a linear function of CA10. Further, CA50 is estimated as

$$CA50 = CA10 + \frac{\Delta\theta}{2}. \qquad (13)$$

Heat Release The heat release due to complete combustion in an adiabatic constant volume process would result in a temperature rise (ΔT_{ad}) as shown in Eq. (14). However, this overestimates the actual temperature rise, and is multiplied with an efficiency term $\eta(CA90, i_c)$ that lumps the cumulative effects of heat losses and combustion efficiency

$$\Delta T_{ad} = \frac{Q_{lhv} m_f(k)}{c_v m_c} \qquad (14)$$

$$T_{CA90} = T_{CA10} + \Delta T_{ad} \cdot \eta(CA90, i_c). \qquad (15)$$

Here Q_{lhv} is the lower heating value of the fuel, while c_v is the heat capacity of the charge at constant volume. Figure 4 shows that the modeled combustion efficiency reduces with increasing i_c and $CA90$. These trends are consistent with Section 2.10.5 of [14]. The temperature and pressure between CA10 and CA90 are calculated by assuming that the temperature rise due to heat release occurs uniformly over the burn duration.

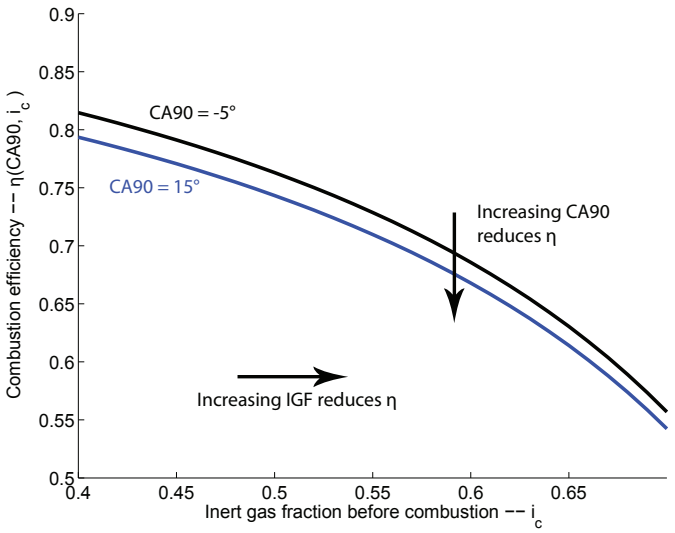

Figure 4. COMBUSTION EFFICIENCY $\eta(CA90, i_c)$

Phase 3: Polytropic expansion followed by blowdown and exhaust After CA90, the mixture expands polytropically to EVO, thus determining T_{evo} and p_{evo}. After EVO, the exhaust temperature of the blowdown gases is considered to be the result of an adiabatic expansion of the gas down to the exhaust manifold pressure, with a polytropic exponent n_{bd}.

$$T_{bd}(k+1) = T_{evo} \left(\frac{p_{em}(k)}{p_{evo}(k)}\right)^{\frac{n_{bd}}{n_{bd}-1}} \qquad (16)$$

Decoupling composition from phasing prediction

The combustion phasing prediction is mainly thermally driven. The only coupling between the composition state and combustion phasing is the efficiency term $\eta(CA90, i_c)$ that modulates the rise in temperature due to combustion. A simplified decoupled model was derived by replacing this with a simplified efficiency term $\eta_1(CA90)$, thus eliminating the influence of composition on combustion phasing prediction. This decoupling is attractive from a control analysis and design perspective.

STEADY STATE VALIDATION

The model parameters were fitted using steady state HCCI dynamometer data from a 2.0 liter four-cylinder gasoline engine with a compression ratio of 10.5. The experiments were carried out at 2000 RPM, while other conditions and actuator values varied as tabulated in Tab. 1. The experimental data were processed by a high-fidelity offline combustion analysis tool provided by Robert Bosch, see [15]. The offline calculations for combustion phasing, in-cylinder residual fraction and temperature, etc. were used to tune and validate the model.

The primary aim of this study is to develop a model suitable for combustion phasing control, and so the main performance

Table 1. EXPERIMENT RANGES

Output / Actuator	Range
CA50	-4.5→10 °CA aTDC
IMEP	1.4→2.7 bar
Fuel Mass	5.8→10.2 mg/cycle
Injection Timing	300→400 °CA bTDC
Throttle	8→100%
Lambda	0.97→1.3

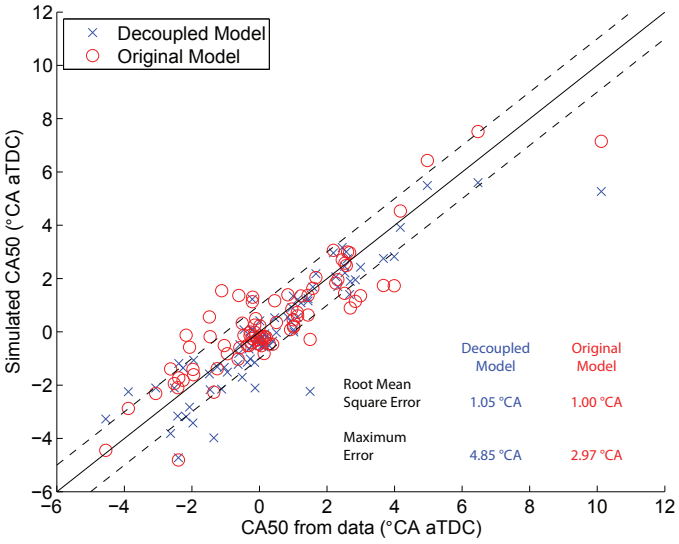

Figure 5. CA50 RESULTS – SIMULATION VS. DATA

output of the model is CA50. Secondary outputs have been validated including charge conditions at IVC and EVO, x_r, and m_c. Figure 5 shows good steady state combustion phasing prediction performance for both the composition-decoupled and the original composition-influenced models. This is further demonstrated in Fig. 6, 7, and 8 where sweeps in fuel mass, fuel injection timing and NVO respectively are considered.

It is seen that steady state performance has been maintained even after decoupling the influence of composition. The steady state prediction of CA50 is comparable for both models, and matches reasonably well with the CA50 predicted by the offline combustion analysis tool. Steady state trends in model variables during various actuator sweeps are predicted well; however differences between the two models in the transient performance are observed and are presented in the following and final section of the paper.

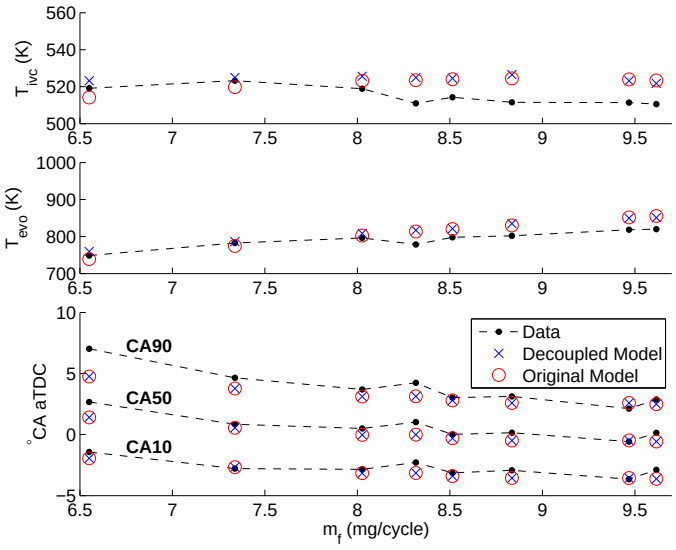

Figure 6. SWEEP IN MASS OF FUEL

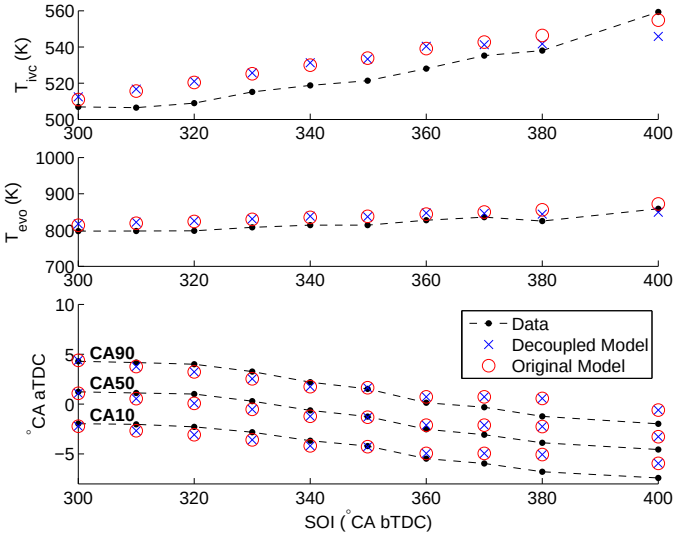

Figure 7. SWEEP IN INJECTION TIMING

TRANSIENT PREDICTIONS

The previous section shows that it is possible to get very comparable steady state performance using either the composition-decoupled or the original composition-influenced model. The transient CA50 evolutions of the two models were compared to determine whether IGF, and hence composition effects, should be kept as a state. Figure 9 shows the transient response of the two models at three different operating points. At each operating point the NVO is stepped down and then back up again by 7°. The most striking difference is the presence of an overshoot in the original composition-influenced model. Behavior similar to the overshoot has been reported, by Shaver et al. in [1].

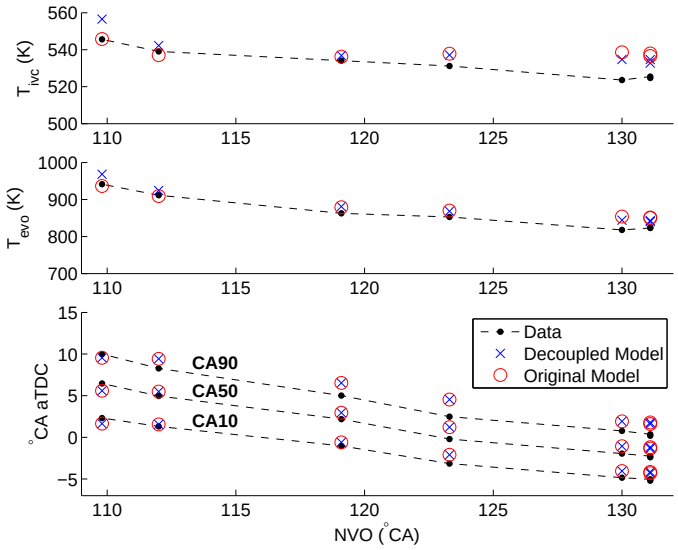

Figure 8. SWEEP IN NVO

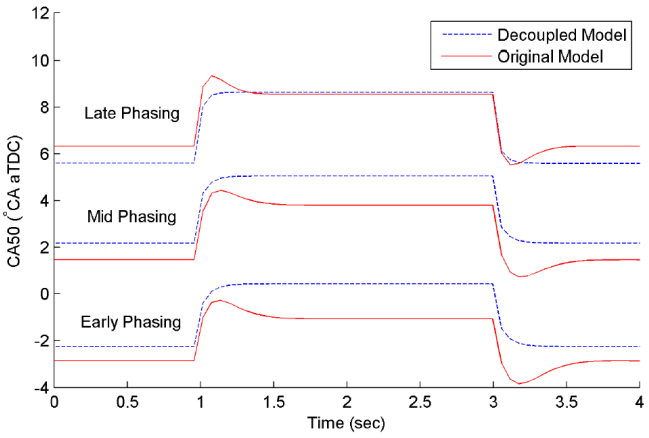

Figure 9. TRANSIENT RESPONSE TO NVO STEP AT EARLY, MID, AND LATE PHASING CONDITIONS

The coupling that leads to overshoot

The overshoots in CA50 seen in Fig. 9 can be explained by the interplay between the faster actuator-driven dynamics of x_r which cause the sharp initial change in T_{ivc} and hence in CA50, and the slower composition-driven dynamics of i_c which cause the slower relaxation to the final steady state CA50 value through its influence on the combustion efficiency.

Figure 10 shows the changes in key intermediate variables in the model following an NVO step. A step down in NVO causes a near instantaneous drop in x_r, and hence in T_{ivc}, consequently retarding CA50. Governed from Eq. (4), i_c decays more slowly to its steady state value. As i_c reduces, η increases, and consequently the temperature of the residuals increase. This leads to slightly higher T_{ivc} which advances CA50 to its final steady state value.

The shape of the transient response is determined by the

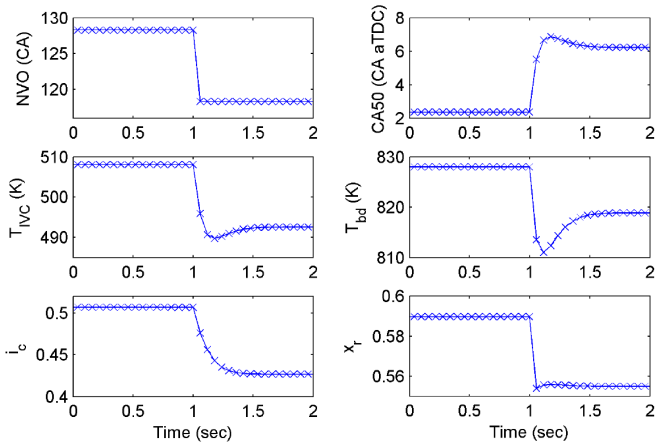

Figure 10. CA50 OVERSHOOT DUE TO COMPETING DYNAMICS

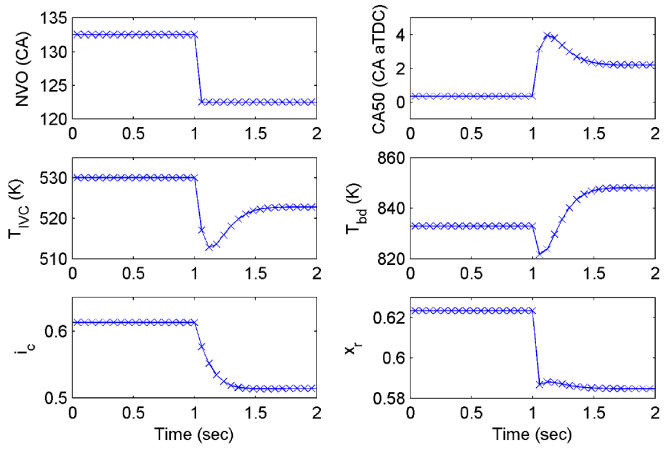

Figure 11. CA50 OVERSHOOT WITH T_{bd} UNDERSHOOT

relative magnitude of the competing effects, which in turn depends nonlinearly on the operating condition. This is demonstrated in Fig. 10 and 11 that show a step in NVO at two different operating conditions. In Fig. 10, the state T_{bd} shows an overshoot whereas a sign reversal and non-minimum phase behavior appear for the step in Fig. 11.

As the coupling between the i_{bd} state and CA50 is only via the combustion efficiency, its shape is very important in determining the dynamical characteristics of the response. This effect of competing dynamics is not captured in the composition-decoupled model, as the efficiency factor η_1 does not depend on IGF. In the operating points considered, damped responses are seen in the composition-decoupled model.

EXTREMELY LATE PHASING CONDITIONS

Despite not being able to model the composition-driven transient overshoots, the decoupled model is able to demonstrate

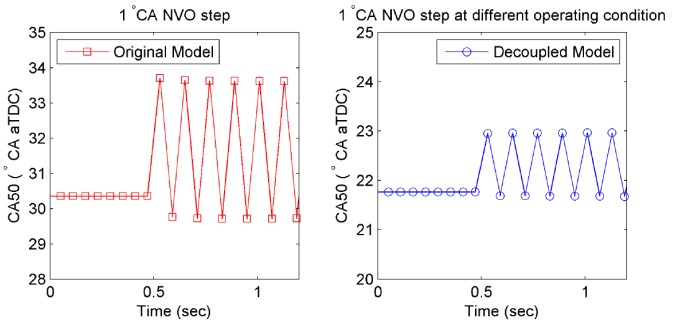

Figure 12. LIMIT CYCLE BEHAVIOR AT EXTREMELY LATE PHASING

complex non-linear dynamical phenomena such as bifurcations yielding limit cycles of period two. These occur at extremely late phasing conditions that form the boundary of the stable operation region for HCCI combustion. An example of such behavior is shown in Fig. 12. The phasing shown in the figure is very close to the misfire region and the engine might stall before the limit cycle is established. However, the qualitative predictions are of greater interest than the quantitative predictions as the model has not been validated by experiments in this region. These nonlinear responses are exhibited by both models at the late phasing conditions, and are currently being investigated. Similar results have been shown in literature, see for example [8, 16, 17].

CONCLUSIONS

A zero-dimensional control-oriented model for recompression HCCI combustion is presented, using a temperature and a composition state. It is shown that the use of inert gas fraction and oxygen mole fraction are equivalent choices for the composition state. This model captures the steady state trends for sweeps in valve timing, fuel mass, and fuel injection timing.

It is observed that the composition influenced model demonstrates overshoots in combustion phasing response over wide operating range. Analysis of this physics-based model shows that the interplay between composition-influenced slow and fast dynamics causes the overshoots in combustion phasing. At certain operating points these competing dynamics cause the state T_{bd} to exhibit non-minimum phase behavior.

Decoupling the composition from the combustion phasing prediction model yields a simpler model that maintains steady-state fidelity, but cannot capture the composition-driven competing dynamics. Both models exhibit complex nonlinear behavior at extreme phasing conditions. Data sets with transient experimental observations are needed to further investigate these phenomena, and conclude on the necessity of including composition effects on the combustion phasing.

ACKNOWLEDGMENT

This material is based upon work supported by the Department of Energy [National Energy Technology Laboratory] under Award Number(s) DE-EE0003533[1]. This work is performed as a part of the ACCESS project consortium (Robert Bosch LLC, AVL Inc., Emitec Inc.) under the direction of PI Hakan Yilmaz, Robert Bosch, LLC.

The authors would like to thank Alexandra Fuchsbauer at Robert Bosch GmbH for several helpful technical discussions.

REFERENCES

[1] Shaver, G. M., Roelle, M. J., Caton, P. A., Kaahaaina, N. B., Ravi, N., Houthout, J.-P., Ahmed, J., Kojic, A., Park, S., Edwards, C. F., and Gerdes, J. C., 2005. "A physics-based approach to the control of Homogeneous Charge Compression Ignition engines with variable valve actuation". *International Journal of Engine Research,* **6**(4), pp. 361–375.

[2] Rausen, D., Stefanopoulou, A., Kang, J.-M., Eng, J., and Kuo, T.-W., Sep. 2005. "A mean value model for control of Homogeneous Charge Compression Ignition (HCCI) engines". *Journal of Dynamic Systems, Measurement, and Control,* **127**(3), pp. 355–362.

[3] Chiang, C., Stefanopoulou, A. G., and Jankovic, M., 2007. "Nonlinear observer-based control of load transitions in homogeneous charge compression ignition engines". *IEEE Transactions on Control Systems Technology,* **15**(3), May, pp. 438–448.

[4] Bengtsson, J., Strandh, P., Johansson, R., Tunestal, P., and Johansson, B., Nov. 2007. "Hybrid modelling of Homogeneous Charge Compression Ignition (HCCI) engine dynamic – a survey". *International Journal of Control,* **80**(11), pp. 1814–1848.

[5] Ravi, N., Liao, H.-h., Jungkunz, A. F., and Gerdes, J. C., 2010. "Modeling and control of exhaust recompression HCCI using split injection". *2010 American Control Conference*.

[6] Chiang, C.-J., and Stefanopoulou, A. G., 2009. "Sensitivity analysis of combustion timing of Homogeneous Charge Compression Ignition gasoline engines". *Journal of Dynamic Systems, Measurement, and Control,* **131**(1), pp. 014506–1 to 014506–5.

[7] Willand, J., Nieberding, R.-G., Vent, G., and Enderle, C., 1998. "The knocking syndrome – its cure and its potential". *SAE International Fall Fuels and Lubricants Meeting and Exhibition,* **982483**.

[8] Hellström, E., Stefanopoulou, A. G., and Vávra, J., 2011.

[1] Disclaimer: This report was prepared as an account of work sponsored by an agency of the United States Government. Neither the United States Government nor any agency thereof, nor any of their employees, makes any warranty, express or implied, or assumes any legal liability or responsibility for the accuracy, completeness, or usefulness of any information, apparatus, product, or process disclosed, or represents that its use would not infringe privately owned rights. Reference herein to any specific commercial product, process, or service by trade name, trademark, manufacturer, or otherwise does not necessarily constitute or imply its endorsement, recommendation, or favoring by the United States Government or any agency thereof. The views and opinions of authors expressed herein do not necessarily state or reflect those of the United States Government or any agency thereof.

"Modeling bifurcations in autoignition combustion". Submitted to IEEE Conference on Decision and Control, 2011.
[9] Daw, C., Edwards, K., Wagner, R., and J.B. Green, J., 2008. "Modeling cyclic variability in spark-assisted HCCI". *Journal of Engineering for Gas Turbines and Power,* **130**(5), p. 052801.
[10] Heywood, J., 1988. *Internal Combustion Engine Fundamentals*. McGraw-Hill Science/Engineering/Math.
[11] Livengood, J., and Wu, P., 1955. "Correlation of autoignition phenomena in internal combustion engines and rapid compression machines". In Symposium (International) on Combustion, Vol. 5, Elsevier, pp. 347–356.
[12] He, X., Donovan, M., Zigler, B., Palmer, T., Walton, S., Wooldridge, M., and Atreya, A., 2005. "An experimental and modeling study of iso-octane ignition delay times under Homogeneous Charge Compression Ignition conditions". *Combustion and Flame,* **142**(3), pp. 266–275.
[13] Mayhew, C. G., Knierim, K. L., Chaturvedi, N. A., Park, S., Ahmed, J., and Kojic, A., 2009. "Reduced-order modeling for studying and controlling misfire in four-stroke HCCI engines". *48th IEEE Conference on Decision and Control*, pp. 5194–5199.
[14] Chiang, C., 2007. "Modeling and control of Homogeneous Charge Compression Ignition engines with high dilution". PhD thesis, University of Michigan.
[15] Kulzer, A., Lejsek, D., and Nier, T., 2010. "A thermodynamic study on boosted HCCI: Motivation, analysis and potential". *SAE Int. J. Engines,* **3**(1), pp. 733–749.
[16] Koopmans, L., and Denbratt, I., 2001. "A four stroke camless engine, operated in homogeneous charge compression ignition mode with commercial gasoline". *SAE World Congress,* **2001-01-3610**.
[17] Ishibashi, Y., and Asai, M., 1996. "Improving the exhaust emissions of two-stroke engines by applying the activated radical combustion". *SAE International Congress and Exposition,* **960742**.

Appendix A: Relationship between i_{bd} and χ_{O_2}

The relationship between IGF state i_{bd} and χ_{O_2} is derived for iso-octane fuel (C_8H_{18}) in Eq. (22), and then extended to a general hydrocarbon C_aH_b in Eq. (24).

Consider Eq. (17) which shows the chemical reaction for the stoichiometric combustion of one mole of C_8H_{18}. From this, the constituents of the in-cylinder charge are considered to be:

1. Fuel (iso-octane) : C_8H_{18}
2. Air : $O_2+3.773N_2$
3. Inert gas mixture : $8CO_2+9H_2O+47.16N_2$

Equation (18) represents the lean combustion considered in this study. Here the coefficient of air in the reactants is $12.5\lambda_c$ where λ_c is the relative AFR before combustion as expressed in Eq. (6), and is greater than 1. The reactants also include $N_{IG,res}$ moles of the inert gas mixture. Complete combustion of the reactants results in $N_{IG,exh}$ moles of the inert gas mixture and $12.5\,(\lambda_c-1)$ moles of air.

$$C_8H_{18}+12.5\,(O_2+3.773N_2)\rightarrow(8CO_2+9H_2O+47.16N_2) \tag{17}$$

$$\begin{aligned}C_8H_{18}+12.5\lambda_c\,(O_2+3.773N_2)+N_{IG,res}(8CO_2+9H_2O\\ +47.16N_2)\rightarrow N_{IG,exh}\,(8CO_2+9H_2O+47.16N_2)\\ +12.5\,(\lambda_c-1)\,(O_2+3.773N_2)\end{aligned} \tag{18}$$

At steady state, Eq. (19) relates the residual gas fraction (x_r) to the ratio of the moles of the inert gas mixture in the residuals and the products. As the composition of the residual gases and the gases after combustion is assumed to be the same, the ratio of the moles is also the ratio of the masses. Further, balancing carbon atoms in Eq. (18) leads to Eq. (20).

$$x_r=\frac{m_{res}}{m_c}=\frac{m_{IG,res}}{m_{IG,exh}}=\frac{N_{IG,res}}{N_{IG,exh}} \tag{19}$$

$$N_{IG,exh}=1+N_{IG,res} \tag{20}$$

The ratio of the number of moles of oxygen to the total number of moles of reactants before combustion is defined as χ_{O_2}. Solving Eq. (19) and (20) determines the unknown coefficients in the combustion equation, as shown in Eq. (21). This leads to the expression for χ_{O_2} in Eq. (22), solely in terms of λ_c and x_r

$$N_{IG,res}=\frac{x_r}{1-x_r};\quad N_{IG,exh}=\frac{1}{1-x_r} \tag{21}$$

$$\chi_{O_2}=\frac{N_{O_2}}{N_{total}}=\frac{12.5\lambda_c(k)}{1+59.66\lambda_c(k)+\frac{64.16x_r(k)}{1-x_r(k)}}. \tag{22}$$

Further, from the expressions for x_r and λ_c given by Eq. (1) and (6) respectively, χ_{O_2} can be calculated from the states and inputs.

Finally, χ_{O_2} can be determined for a general hydrocarbon C_aH_b using Eq. (24), where the coefficients of Eq. (22) depend on a and b. In the expression for λ_c given by Eq. (6), the stoichiometric AFR (AFR_s) will be given by

$$AFR_s=\frac{\left(a+\frac{b}{4}\right)(32+3.773\cdot 28)}{12a+b} \tag{23}$$

$$\chi_{O_2}=\frac{\lambda_c(k)\left(a+\frac{b}{4}\right)}{1+4.773\lambda_c(k)\left(a+\frac{b}{4}\right)+\frac{x_r(k)}{1-x_r(k)}\left(a+\frac{b}{2}+3.773\left(a+\frac{b}{4}\right)\right)}. \tag{24}$$